Journal of Materials Chemistry A

Accepted Manuscript

ROYAL SOCIETY OF CHEMISTRY

www.rsc.org/materialsA

Formation Mechanism of Layered Double Hydroxide Nanoscrolls by Facile Trinal-Phase Hydrothermal Treatment and Their Adsorption Properties

Weiyang LV, Miao DU*, Weijuan YE, Qiang ZHENG

MOE Key Laboratory of Macromolecular Synthesis and Functionalization, Department of Polymer Science and Engineering*, Zhejiang University, Hangzhou, 310027, China*

Abstract: The formation mechanism of layered double hydroxide (LDH) nanoscrolls via a trinal-phase hydrothermal system has been investigated via powder X-ray diffraction and transmission electron microscopy (TEM) at different reaction temperatures and times. LDH nanosheets formed at first and subsequently developed into nanoscrolls. Notably, the investigation confirmed that urea and pressure played key roles in the formation of the one-dimensional LDH structure. Further observations by scanning electron microscopy and high-resolution TEM indicated that the nanoscrolls with apparent hollow cores derived from nanosheets through a roll-up process, rather than through the control of the crystal growth in one particular direction. A detailed model was also proposed to describe the reaction process based on the assumption that the LDH growth units are anion coordination octahedrons. Furthermore, owing to the increased specific surface area and novel structure, the nanoscrolls exhibit high adsorption capacity and excellent reusability in the adsorption of methyl orange in aqueous solution.

Keywords: Layered double hydroxides, nanoscrolls, roll-up, adsorption

*Corresponding author. E-mail: dumiao@zju.edu.cn, Tel.&Fax: 0086-571-87953075

Introduction

Layered double hydroxides (LDHs) are known as hydrotalcite-like compounds and comprise a large family of lamellar materials with positively charged layers; they have received considerable attention because of their superior interlayer ion exchange properties, high specific surface area, and photocatalytic activities, which are advantageous for anion exchange, magnetic, absorption, catalysis, and medicine applications[1-6]. To achieve these functions, the morphology control and homogeneous dispersion in a medium are the key factors that have received considerable attention due to their significant influence on the material properties[7]. Over the past two decades, many LDHs with one-dimensional (1D; belt-like, wire, and rod-like[8, 9]), two-dimensional (2D; flake-like[10]), and three-dimensional (3D; honeycomb-like[11]) morphologies have been reported. Among them, 1D-LDHs have received considerable attention because of their superior potential in filler orientation during composite fabrication, which results in the enhancement of the mechanical and electrochemical properties[12]. Co-precipitation methods (constant-pH or variable-pH), hydrothermal treatment, and reverse microemulsion methods are all employed to fabricate 1D-LDHs. However, the products obtained by these conventional methods contain only a small amount of 1D-LDHs, which generally show a paragenetic relationship with 2D-LDH nanosheets, usually leading to large aggregates[8, 13, 14] and therefore causing poor dispersion in the medium (solvent or polymer matrix). Furthermore, although a variety of LDHs have been fabricated by utilizing various reactions, the formation mechanism of 1D-LDHs (nanofibers, nanosticks, nanotubes)

remains undetermined, which extremely hinders the effective fabrication of 1D-LDH structures and morphologies as well as their application.

Hydrothermal treatment in an autoclave at high temperatures usually leads to a more even distribution of cations in the hydroxide layers, more regular crystallite shapes, and growth of individual crystallites via cation diffusion and crystallite ripening[15]. Generally, the reactants in the hydrothermal autoclave have only one phase, i.e., the salt aqueous solution, and the obtained 1D-LDHs are often symbiotic with the nanosheets[13]. On the other hand, although reverse emulsion systems at normal pressure have been used to fabricate LDHs with different morphologies, pure and homogeneously dispersed 1D-LDHs can be hardly obtained[14]. The reverse microemulsion crystallizing in the hydrothermal autoclave can lead to the formation of LDH nanowires[9]. However, the reverse microemulsion has been reported to be unstable in an autoclave without stirring, as its water/oil ratio is close to the critical value[16].

In this paper, an extremely large amount of surfactants were introduced to prepare the salt (divalent and trivalent metal cations) aqueous solution and alkali reagent aqueous solution form a nanoscale phase (the phase size is smaller than 100 nm) within the oil phase. Hydrothermal treatments at relatively high temperature were then performed. Surprisingly, a novel morphology of 1D-LDHs, named as nanoscrolls and thoroughly different from the reported nanowires, was obtained. Here, a distinctive nanosheet roll-up mechanism is proposed: nanosheets form at first and then develop into nanoscrolls; in other words, the ultimate 1D-LDH is actually

derived from a lamellar structure. To distinguish it from the other reported methods, the technique employed in this paper was termed as trinal-phase hydrothermal treatment. The trinal-phase comprises a salt aqueous solution phase, alkali reagent aqueous solution phase, and oil phase. In addition, the as-obtained LDH nanoscrolls possess an extremely high specific surface area and exhibit excellent performance for adsorbing methyl orange in aqueous solution.

Results and discussion

Time evolution of the LDH morphology

The morphological time (t) evolution and X-ray diffraction (XRD) patterns of LDHs prepared at 110 °C are displayed in Fig. 1. At t = 6 h, LDH nanosheets with irregular edges could be observed, as shown in Fig. 1a. Some of them rolled up from the foreland of the nanosheets, which were considered to be the embryo of the 1D-LDH nanoscrolls. Surprisingly, the LDH nanosheets disappeared with the increase of the reaction time, i.e., at t = 12 h, and only 1D-LDHs could be observed (Fig. 1b). Likely, most of the 2D nanosheets rolled up to form much more mature nanoscrolls. The as-synthesized nanoscrolls have an external diameter of approximately 30–100 nm and length of around 1–2 μm. The thickness of the sample was tested by AFM, which is about 46 nm (Fig. S1). When the aging time was further increased to 24 h, some LDH nanoscrolls were destroyed, and the nanosheets appeared again, as shown in Fig. 1c; this phenomenon can be attributed to the further hydrolysis of urea and the oxidation of LDH at high pressure. Fig. 1d shows the time evolution of the XRD

patterns of the LDHs. The LDHs synthesized at t = 6 h exhibit the characteristic reflections corresponding to the (003), (006), and (009) planes of Co-Al-SO_4-LDH. Nevertheless, the large half width of the (003) diffraction peak (approximately 4°) implies the imperfect crystallization of the LDHs. Bragg reflections indexed as (003) with the interlayer anion of SO_4^{2-} were observed at 2θ = 8.3°, indicating that the interlayer distance between the LDH layers was 1.078 nm. At t = 12 h, a relatively sharp (003) diffraction peak appeared (approximately 1.1°), indicating the achievement of a perfect LDH crystal. When the reaction time reached 24 h, the products exhibited not only the characteristic reflections of Co-Al-SO_4-LDH crystals, but also some diffraction peaks of the composite oxide (2θ of 31.3°, 36.5°, 44.6°, 59.1°, 65.2°). Compared with the pattern of the sample at 12 h, a strong diffraction peak was observed at 2θ = 11.6°, implying that the CO_3^{2-} ion generated by urea had already partly intercalated into the LDH layers, and the corresponding interlayer distance was only 0.75 nm. Such a small interlayer spacing, compared with that of SO_4^{2-} as interlayer anion, suggests a stronger electrostatic interaction between the LDH layers[17]. In this case, the LDH 1D structure becomes unstable because of the rising elastic strain energy resulting from the bent crystal plate, which causes the outspreading of the LDH nanoscrolls[18]. Clearly, the LDH morphology strongly depends on the reaction time, and only proper conditions can lead to the formation of the nanoscrolls. Under hydrothermal conditions, the growth mechanism of the LDH crystals involved the formation of 2D nanosheets at first, and then their conversion into 1D nanoscrolls. These findings differ from previous results[9] according to which,

at t = 6 h, smaller nanowires were obtained instead of nanosheets. Such significant dimensional differences might be ascribed to the remarkable difference in metallic elements and formation mechanisms.

For the remainder of this study, the reaction time was fixed at 12 h for convenience.

Effect of aging temperature on the LDH morphology

The effect of the hydrothermal treatment temperature on the formation of the LDH nanoscrolls was investigated. As shown in Fig. S2, the LDH nanoscrolls and nanosheets coexisted in the product synthesized at 100 °C (the corresponding saturated vapor pressure for the mixed solvent was approximately 0.16 MPa), whereas pure, uniform, and perfect nanoscrolls were obtained at 110 °C, as the relatively high vapor pressure (approximately 0.21 MPa at 110 °C) resulting from the increased temperature weakened the electrostatic forces between the LDH layers[13] and facilitated the roll-up activity of the LDH nanosheets. When the temperature was further increased to 120 °C, the nanoscrolls disappeared and were replaced by large LDH aggregations containing some oxidized composites, as confirmed by the XRD results (Fig. S2d). Although the high vapor pressure (approximately 0.28 MPa at 120 °C) promoted the nanoscroll formation, the high temperature facilitated the urea hydrolysis, forming CO_3^{2-}. Thus, the reason behind the reappearance of the LDH nanosheets at high temperature may be the same as discussed above, that is, the 1D-LDH structures become unstable with the presence of CO_3^{2-} as the interlayer

anion, outspreading the LDH nanoscrolls again. These results demonstrate that prolonging the reaction time and increasing the temperature have the same effect on the morphology of Co-Al-LDHs.

Effect of alkali reagent on the LDH morphology

Alkali reagents play a major role in fabricating LDH nanoscrolls. The conventional alkali reagent, sodium hydroxide (NaOH), was first selected. However, rather than nanoscrolls, LDH nanosheets were fabricated regardless of the short or long reaction time (Fig. 2a). The nucleation and growth of the LDH crystals are probably too fast, leading to the LDH nanosheets only with the lateral size of 50 nm, which is far more difficult to roll up. Compared with a NaOH solution, an aqueous urea solution is weakly alkaline. At higher temperatures, urea would hydrolyze and gradually release OH^- and CO_2, making the ultimate aqueous solution weakly alkaline. The appropriate hydrolysis rate of urea provides enough time and alkalinity for the growth and roll-up of the 2D-LDH nanosheets, which is controlled by the reaction temperature and time. As shown in Fig. 2b, nanoscrolls were obtained as well as nanosheets, confirming the crucial role of urea in the nanosheet rolling process. Notably, conventional hydrothermal treatment systems (one phase) with urea as the alkali reagent could not produce uniform 1D-LDHs. When the conventional hydrothermal treatment system was replaced by a trinal-phase hydrothermal treatment with all the other conditions unchanged, uniform and homogeneously dispersed nanoscrolls could be obtained (Fig. 2c), implying that, besides the alkali reagent, the

trinal-phase also plays a key role to fabricate pure 1D-LDH nanoscrolls.

The synthesis of the LDHs shown in Fig. 2d was conducted in a three-neck flask under a nitrogen flow at a temperature of 97 °C. The experiment was therefore performed under atmospheric pressure, and LDH sheets with a lateral size in the order of micrometers were obtained, as previously reported in the literature[1]. Thus, the pressure also strongly influences the LDH morphology, and only the coexistence of urea and high pressure can lead to the formation of LDH nanoscrolls.

Therefore, proper aging temperature (higher pressure), relatively longer aging time, use of urea, and a trinal-phase system can facilitate the formation of 1D structures. The slow hydrolyzation of urea provides enough time for the growth of the LDH crystals, while the trinal-phase system, with salt and alkali reagent aqueous solutions as dispersion phases, prevents the aggregation of the LDHs, ensuring the synthesis of uniform nanoscrolls.

To gain insights into the structure of the LDH nanoscrolls, scanning electron microscopy (SEM) and high-resolution transmission electron microscopy (HRTEM) images of the samples obtained at 110 °C and t = 12 h were analyzed. SEM image showing the overall morphology of the products was given in Fig. S3. Fig. 3a shows LDH flower-like aggregates with some vertically aligned scrolls; this structure allows viewing the sample from the direction of the tubular axis. Hollow cores can be observed in the magnified image, as indicated by the arrows in Fig. 3b. This phenomenon indubitably demonstrates that the 1D-LDH evolution entails the initial formation of a lamellar structure followed by a roll-up process, rather than the control

of the crystal growth in one particular direction; this formation mechanism, also confirmed by the TEM observations (Fig. 3c and d), is entirely different from the process previously reported[9, 14]. The nanoscrolls were further examined by HRTEM, as shown in Fig. 3e and f. Generally, nanotubes can be structurally divided into nesting and scroll types[19]. The nesting type has the same number of layers on both sides, whereas the scroll type lacks one layer on one side. Clearly, the 1D-LDHs obtained here belong to the latter type. The HRTEM image reveals that the spacing between the adjacent layers of the nanoscroll wall is 1.03 nm, which is consistent with the value of the interlayer distance calculated by XRD (1.078 nm). This finding indicates that the nanosheets roll up to gain stabilization energy when counterparts to form a stack structure cannot be found.[20] A selected area electron diffraction (SAED) pattern of the nanoscroll is shown in Fig. 3f. The reflections can be indexed by a hexagonal unit cell with unit cell parameters of approximately a = b = 0.271 nm, which within the errors of the values (a = b = 0.286 nm) determined by XRD.

Formation mechanism of the LDH morphology

On the basis of the above results, the formation mechanism of the LDH nanoscrolls in the present study is schematically illustrated in Scheme 1. Until now, the accurate LDH layers of a nanosheet that can be rolled into nanoscroll are unclear; therefore, hereafter, the nanosheets able to roll will be denoted as “flexible laminates” for clarity. The two different aqueous phases containing the metal ions and urea were dispersed in the oil phase to form droplets surrounded by cetyltrimethylammonium

bromide (CTAB) and *n*-hexanol. A coalescence and decoalescence of the droplets occurred, causing the consequent exchange of nutrients for the growth of the LDHs. As the temperature increased, urea began to decompose and the OH^- ions diffused into the salt aqueous phase, followed by the nucleation of the LDH. It was reported that the growth units of the LDHs were anion coordination octahedrons[21], which could be formulated as $[Co(Al)\text{-}(OH)_6]^{4(3)-}$ in this study. Droplets surrounded by CTAB possessed positive charges, so the negatively charged growth units could be attracted to the electric double layer at the interfaces through electrostatic interaction. As a result, the growth of the LDH layer was favored along the interface, ensuring the synthesis of a flexible laminate. To verify the proposed assumption, sodium dodecyl sulfate (SDS) was used as the contrastive surfactant in the reaction system, in which oppositely charged droplets can be formed. Owing to the electrostatic repulsion between the growth units and the interface, the droplets acted as homogeneous microreactors without further restrictions for the crystallization of LDHs, leading to the formation of LDH nanosheets with small lateral sizes, as shown in Fig. S4. Obviously, once the flexible laminate was formed, it was active and tended to flocculate within itself to maintain its stability, starting the roll-up process. With the assistance of high pressure, as discussed above, the flexible laminate successfully rolled up into a nanoscroll.

For a typical LDH stack structure, the value of *d*(003) in the XRD pattern indicates the interlayer distance between adjacent nanosheets. In this study, the spacing between the adjacent layers of the nanoscroll wall is consistent with that of

the stack structure, indicating that the roll-up behavior plays the same role as the stacking in keeping the stability of the LDH nanosheet. In other words, depending on the specific environment, the stable multilayered structure can be achieved through either the stacking of tens of LDH layers or the rolling of the flexible laminate.

Adsorption properties of the LDH nanoscrolls

To fathom the textural properties of the LDHs synthesized in this work, N_2 adsorption experiments were performed. As shown in Fig. 4, each LDH synthesized using either conventional urea release or the trinal-phase hydrothermal treatment exhibits the typical isotherm of type Π according to the IUPAC classification, which is characteristic of the nitrogen adsorption on macroporous samples. The pore size curves also confirm that the LDH products mainly consist of meso and macropores. Moreover, the hysteresis loops of these isotherms are of type H3, which is often given by aggregates of plate-like particles or by adsorbents exhibiting slit-shaped pores[22]. Obviously, the LDH synthesized by the urea releasing method is part of the former conditions, whereas the nanoscrolls belong to the latter. Interestingly, the two LDH samples exhibt an approximately similar pore size distribution, and a sharp peak centered around 7 nm observed in nanoscrolls demonstrates that more internal structure has been exposed to outside during rolling process compared with the nanosheets, which provides further powerful evidence of the formation mechanism of the LDH nanoscrolls, as the surface properties remain consistent, indicating that the 1D structure is derived from the LDH nanosheets.

Table 1 summarizes the structural parameters of the LDH samples; both the surface area and pore volume of the LDH nanoscrolls exhibit a fourfold increase compared with those of the nanosheets, which can be ascribed to the different stacking patterns. This fascinating observation may help us produce LDH nanoscrolls as excellent absorbents in solving water pollution problems.

In this study, methyl orange (MO) dye was selected as a type of water pollutant to test the adsorption properties of the LDH nanoscrolls. The adsorption kinetics of LDH samples towards MO was explored, and the data are fitted by using three kinetic models (the pseudo-first-order, the pseudo-second-order and the Elovich models). The adsorbed amount of LDH samples at different time can be well fitted by the pseudo-second-order as shown in Fig.5a, indicates that the rate limiting step in the adsorption process involves chemisorption of MO on LDHs[23], and the equilibrium adsorption of the two LDH samples can reach 70% within 10 min. The calculated kinetics parameters of the three models are shown in Table S1. Higher pseudo-second-order rate constant implies the higher MO adsorption rate for LDH nanoscrolls than that for LDH nanosheets.

The equilibrium adsorption of MO for LDH samples has also been tested, and the results are fitted with two important isotherm models (Langmuir and Freundlich) to identify a suitable model for conducting the adsorption process. The calculated Langmuir and Freundlich model parameters and linearization coefficients are given in Table S2. The adsorption data fitted both models very well. Fig. 5b shows that when the initial concentration of MO is 900 mg/L, the adsorption capacity of the LDH

nanoscrolls is 1130 mg/g, which is higher than the values in the range of 85–528 mg/g previously reported[24-28]; compared with the nanosheets in this work, this value also shows a threefold increase. Generally, the promising potential application of LDH in the adsorption of dye anions is due to its high surface area and anion exchange property[29, 30]. For the former, LDH nanosheets comprise tens or hundreds of layers in their stack structure, while the nanoscrolls can only be formed through the laminates that are flexible enough, suggesting that the same LDH layers in one stack structure can roll up into a considerable number of nanoscrolls, and the increased adsorption surface will certainly lead to the improvement of the adsorption properties. For the latter condition, nanoscrolls with few layers can improve the efficiency of the intercalation process during the adsorption, as the layers located near the outer edges of the crystallite are more loosely bound to each other than those found within the bulk of the crystallite[31].

The regeneration always determines the feasibility of applying the adsorbent systems in large-scale operations. In this work, sulfate radical-based advanced oxidation technology was applied for regeneration of the spent samples due to its high efficiency, low cost and fast reaction kinetics of the catalytic process[32-34]. Generally, oxone and homogeneous Co^{2+} were used as the oxidant and catalyst, respectively. In our system, no extra Co^{2+} was added as the LDH nanoscrolls have already contained this element, which could certainly avoid the secondary pollution. The removal percentages of MO by using the same recycled sample are presented in Fig. 6a. It can be seen that more than 90% of dye removal was still retained after three runs, and the

lower removal efficiency compared with the first adsorption process might be ascribed to the LDH wastage during centrifugation and the incomplete degradation. That is to say, the adsorption efficiency of MO decreased from 98.87% to 90.02% even for the third regeneration cycle, indicating the high adsorption capacity of adsorbent for MO was well restored.

Conclusions

In summary, we have demonstrated a detailed mechanism for the growth of LDH nanoscrolls with external diameters of approximately 20–50 nm and lengths of 1–2 μm in a trinal-phase hydrothermal system. During the synthetic process, LDH nanosheets were formed at first, and then developed into 1D structures. Urea and pressure played key roles in promoting the rolling process, while the function of the trinal phase was to prevent the aggregation of the LDHs, ensuring the synthesis of uniform nanoscrolls. Moreover, we have experimentally validated the similar spacing between the nanoscroll walls and the interlayer distance, which means that the LDH multilayered structure can be realized through either a roll-up or a stacking process. Owing to the increased specific surface area and novel structure, the nanoscrolls have an equilibrium adsorption capacity of 1130 mg/g and exhibit a higher MO adsorption capacity than other reported LDH samples. By using the sulfate radical-based advanced oxidation method, the spent LDH samples could be regenerated and more than 90% of dye removal was still retained after three runs. We believe that the findings presented in this study advance the knowledge of the nanoscroll formation

mechanism and extend the application of LDHs to the solution of water pollution issues.

Experimental

Material

Cetyltrimethyl ammonium bromide (CTAB), sodium dodecyl sulfate (SDS), oxone ($2KHSO_5 \cdot KHSO_4 \cdot K_2SO_4$, 4.7% active oxygen), cobalt sulfate heptahydrate, aluminum sulfate octadecahydrate, urea, and n-hexane were purchased from Sinopharm Chemical Reagent Co., Ltd., China. N-hexanol and methyl orange (MO, 96% purity) was supplied by the Aladdin reagent (Shanghai, China). Distilled water was used in the experiments. All the reagents were used as received without further purification.

Preparation of LDH nanoscrolls

As a quaternary microemulsion, CTAB/*n*-hexanol/*n*-hexane/water were selected to synthesize the Co/Al-LDH. For a typical synthesis process, a solution was prepared by dissolving 10 g of CTAB in 10 mL of *n*-hexanol; then, when the solution became transparent, 40 mL of *n*-hexane was added. Next, 5 mL of a 0.1 M solution containing the sulfates of the elements (molar ratio of Co:Al = 3:1) was added into the initial mixture first, where the microemulsion only containing the salt aqueous solution phase was obtained. 5 mL of a 0.9 M urea aqueous solution was then added into the microemulsion subsequently to form the alkali reagent aqueous solution phase, followed by substantial stirring for 1 h; the resulting mixture was transferred to a 100

ml stainless Teflon-lined autoclave and heated at 110 °C for 12 h before being cooled to room temperature. The as-obtained precipitate was centrifuged (at 12000 rpm under 20 °C for 10 min) and washed with ethanol and water several times. The final products were treated using a freeze-drying method.

Characterization

Powder XRD patterns were recorded on a Rigaku D/max 2550 diffractometer (Shimadzu Corporation, Kyoto, Japan) under the following conditions: 40 kV, 300 mA, Cu Ka radiation (λ = 0.1542 nm).

The morphology and size of the products were observed by TEM (JEOL, JEM-1200EX, Japan) and SEM (Hitachi S-4800, Japan). HRTEM characterization was performed on a TEM (JEOL 2100F, Japan) with an accelerating voltage of 200 kV. All the LDH samples were ultrasonically dispersed in ethanol for 1 h before being transferred to the microscope.

AFM imaging (SPI3800N, SII Nano Technology Inc., Japan) was performed in tapping mode by depositing the LDH suspension on mica.

N_2 adsorption-desorption isotherms were measured with a Quantachrome Autosorb-1-c system. The samples were outgassed at 100 °C for 2 h before measurement. The specific surface area was calculated by the BET equation based on the N_2 absorption isotherm, and the BJH method was used to calculate the pore size distribution based on the N_2 adsorption isotherm.

The adsorption experiments were performed as follows. Approximately 6 mg of LDH samples and 10 mL of MO aqueous solution with initial concentration ranging

from 60 mg/L to 900 mg/L were added to a 25 mL conical flask. The oscillation treatment was conducted at 200 r/min and 30 °C for 7 h. The adsorption kinetics experiments were performed using the initial MO concentration of 300 mg/L with the other conditions kept identical to the equilibrium adsorption tests. The concentration of MO remaining in solution was analyzed by a Lambda 35 UV-vis absorption spectrometer at room temperature.

The regeneration process was performed as follows: 60 mg LDH nanoscrolls were added into 100 mL of MO solution (100 mg/L), oscillation treatment was conducted at 200 r/min and 30 °C for 7 h. After adsorption, the LDHs were collected through centrifugation and then dispersed into 50 mL of distilled water. The oxidant, 15 mg of oxone was added into the mixture to degrade the adsorbed MO, followed by stirring for 5 min. Afterwards, the LDHs were centrifuged and washed with distilled water several times for the next run.

Acknowledgements

This work was supported by the National Natural Science Foundation of China (Key Program, Grant 51333004).

References

1 Z. P. Liu, R. Z. Ma, M. Osada, N. Iyi, Y. Ebina, K. Takada and T. Sasaki, *J. Am. Chem. Soc.*, 2006, **128**, 4872-4880.

2 D. Y. Wang, F. R. Costa, A. Vyalikh, A. Leuteritz, U. Scheler, D. Jehnichen, U. Wagenknecht, L. Haussler and G. Heinrich, *Chem. Mat.*, 2009, **21**, 4490-4497.

3 A. N. Ay, B. Zumreoglu-Karan, A. Temel and V. Rives, *Inorg. Chem.*, 2009, **48**, 8871-8877.

4 H. W. Olfs, L. O. Torres-Dorante, R. Eckelt and H. Kosslick, *Appl. Clay Sci.*, 2009, **43**, 459-464.

5 Y. H. Xu, H. Zhang, X. Duan and Y. P. Ding, *Mater. Chem. Phys.*, 2009, **114**, 795-801.
6 Y. E. Miao, H. Zhu, D. Chen, R. Y. Wang, W. W. Tjiu and T. X. Liu, *Mater. Chem. Phys.*, 2012, **134**, 623-630.
7 Y. G. Sun and Y. N. Xia, *Science*, 2002, **298**, 2176-2179.
8 G. Hu and D. O'Hare, *J. Am. Chem. Soc.*, 2005, **127**, 17808-17813.
9 H. Y. Wu, Q. Z. Jiao, Y. Zhao, S. L. Huang, X. F. Li, H. B. Liu and M. J. Zhou, *Mater. Charact.*, 2010, **61**, 227-232.
10 G. Hu, N. Wang, D. O'Hare and J. J. Davis, *J. Mater. Chem.*, 2007, **17**, 2257-2266.
11 E. Geraud, S. Rafqah, M. Sarakha, C. Forano, V. Prevot and F. Leroux, *Chem. Mat.*, 2008, **20**, 1116-1125.
12 J. Memon, J. H. Sun, D. L. Meng, W. Z. Ouyang, M. A. Memon, Y. Huang, S. K. Yan and J. X. Geng, *J. Mater. Chem. A*, 2014, **2**, 5060-5067.
13 L. L. Ren, J. S. Hu, L. J. Wan and C. L. Bai, *Mater. Res. Bull.*, 2007, **42**, 571-575.
14 J. He, B. Li, D. G. Evans and X. Duan, *Colloid Surf. A-Physicochem. Eng. Asp.*, 2004, **251**, 191-196.
15 Z. P. Xu, G. S. Stevenson, C. Q. Lu, G. Q. M. Lu, P. F. Bartlett and P. P. Gray, *J. Am. Chem. Soc.*, 2006, **128**, 36-37.
16 N. Wang, L. J. Yang, L. X. Chen and R. Xiao, *Micro Nano Lett.*, 2014, **9**, 302-307.
17 L. M. Parker, N. B. Milestone and R. H. Newman, *Ind. Eng. Chem. Res.*, 1995, **34**, 1196-1202.
18 S. Zhang, L. M. Peng, Q. Chen, G. H. Du, G. Dawson and W. Z. Zhou, *Phys. Rev. Lett.*, 2003, **91**.
19 R. Z. Ma and T. Sasaki, *Top. Appl. Phys.*, 2010, **117**, 135-146.
20 R. Z. Ma, Y. Bando and T. Sasaki, *J. Phys. Chem. B*, 2004, **108**, 2115-2119.
21 J. S. Wu, Y. K. Xiao, J. Y. Wan and L. R. Wen, *Sci. China-Technol. Sci.*, 2012, **55**, 872-878.
22 M. D. Martinez-Ortiz, E. Lima, V. Lara and J. M. Vivar, *Langmuir*, 2008, **24**, 8904-8911.
23 I. Emmanuelawati, J. Yang, J. Zhang, H. W. Zhang, L. Zhou and C. Z. Yu, *Nanoscale,* 2013, **5**, 6173-6180
24 D. Chen, Y. Li, J. Zhang, J. Z. Zhou, Y. Guo and H. Liu, *Chem. Eng. J.*, 2012, **185**, 120-126.
25 P. Monash and G. Pugazhenthi, *Environ. Prog. Sustain. Energy*, 2014, **33**, 154-159.
26 Z. M. Ni, S. J. Xia, L. G. Wang, F. F. Xing and G. X. Pan, *J. Colloid Interface Sci.*, 2007, **316**, 284-291.
27 Z. Yang, S. S. Ji, W. Gao, C. Zhang, L. Ren, W. W. Tjiu, Z. Zhang, J. S. Pan and T. X. Liu, *J. Colloid Interface Sci.*, 2013, **408**, 25-32.
28 L. Zhang, Y. Tang, L. Zhang and J. Yan, *Journal of Functional Materials*, 2012, **43**, 2469-2472.
29 A. I. Khan and D. O'Hare, *J. Mater. Chem.*, 2002, **12**, 3191-3198.
30 E. Alvarez-Ayuso and H. W. Nugteren, *Water Res.*, 2005, **39**, 2535-2542.
31 E. LopezSalinas, M. GarciaSanchez, J. A. Montoya, D. R. Acosta, J. A. Abasolo and I. Schifter, *Langmuir*, 1997, **13**, 4748-4753.
32 C. P. Chen, P. Gunawan and R. Xu, *J. Mater. Chem.,* 2011, **21**, 1218-1225.
33 W. Zhang, H. L. Tay, S. S. Lin, Y. S Wang, Z. Y. Zhong and R. Xu, *Appl. Catal., B,* 2010, **95**, 93-99.
34 X. Y. Chen, J. W. Chen, X. L. Qiao, D. G. Wang and X. Y. Cai, *Appl. Catal., B,* 2008. **80,** 116-121.

Figures and tables caption

Fig. 1 TEM micrographs of the LDH synthesized at different times: (a) 6 h; (b) 12 h; (c) 24 h and (d) their corresponding XRD patterns.

Fig. 2 TEM micrographs of the LDH synthesized via conventional hydrothermal treatment with (a) NaOH and (b) urea; (c) trinal phase hydrothermal system with urea; (d) conventional urea releasing method.

Fig. 3 Different micrographs of the LDH synthesized at 110 °C for 12 h: (a) SEM; (b) magnified SEM image of the dashed-square region in (a); (c,d) TEM; (e) HRTEM; (f) magnified HRTEM image of the dashed-square region in (e). The inset in (f) is an SAED pattern of the nanoscrolls.

Fig. 4 Nitrogen adsorption-desorption isotherms of the LDH synthesized via (a) conventional urea releasing method and (b) trinal-phase hydrothermal system. The insets in (a) and (b) are the pore size distribution of the two samples.

Fig. 5 (a) MO uptake (300 mg/L at time zero) by LDH nanosheets and nanoscrolls as a function of time at 30 °C. The symbols are for the experimental data, and the curves were calculated by fitting the data according to the pseudo-second-order model; (b) adsorption isotherms of MO dye on LDH nanosheets and nanoscrolls at 30 °C.

Fig. 6 (a) The removal efficiency of MO by adsorption using the LDH nanoscrolls in different recycle runs; (b) Optical image taken after MO dye adsorption with the different recycle runs.

Table 1 Textural properties of the LDH samples synthesized via two methods.

Scheme. 1 Schematic representation of the nucleation and structural evolution process of the LDH nanoscrolls.

Fig. S1 AFM image of the LDH nanoscrolls deposited on mica from ethanol suspension. The curve is the corresponding cross-sectional data along the white line in the image.

Fig. S2 TEM micrographs of the LDH synthesized at different temperatures: (a) 100 °C; (b) 110 °C; (c) 120 °C and (d) their corresponding XRD patterns.

Fig. S3 SEM image of the LDH nanoscrolls synthesized at 110 °C for 12 h.

Fig. S4 TEM micrograph of the LDH synthesized using the SDS as the surfactant in microemulsion.

Table. S1 Kinetic parameters of MO (300 mg/L at time zero) on LDH adsorbents at 30 °C.

Table. S2 Adsorption isotherm parameters of methyl orange dye on LDH adsorbents at 30 °C.

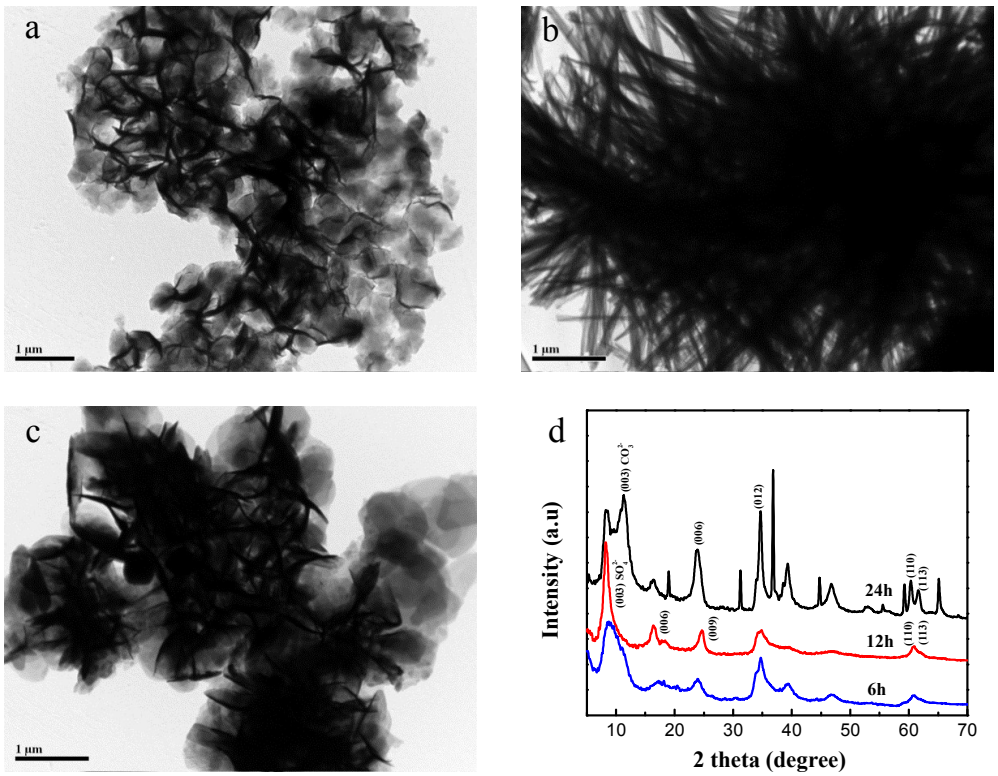

Fig. 1 TEM micrographs of the LDH synthesized at different times: (a) 6 h; (b) 12 h; (c) 24 h and (d) their corresponding XRD patterns.

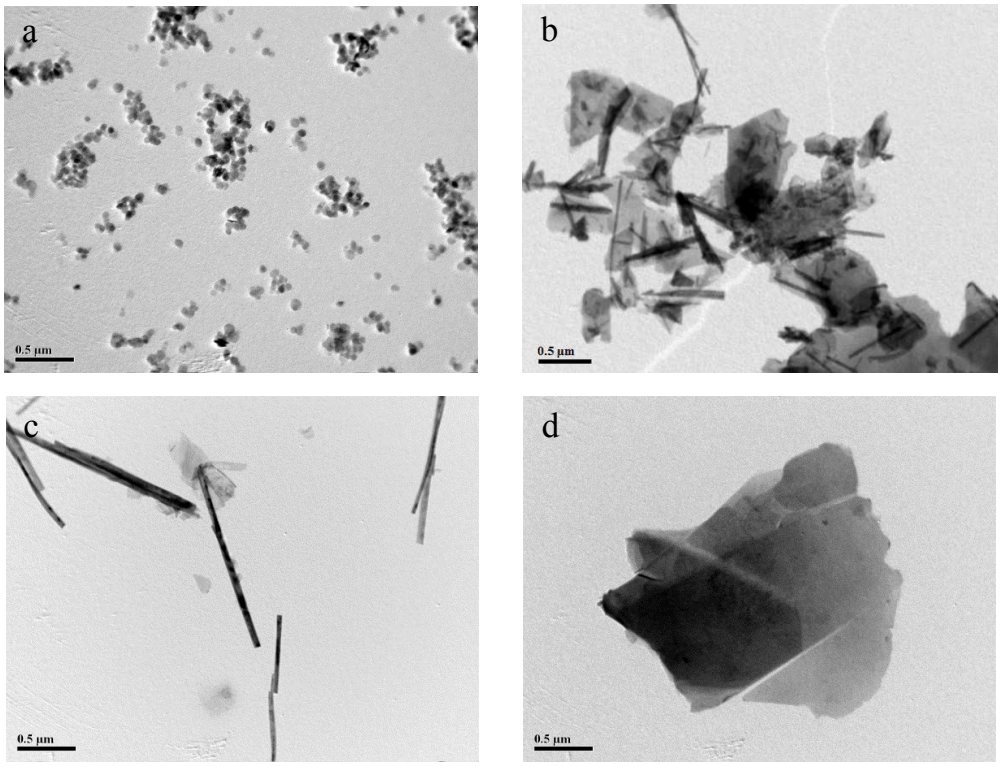

Fig. 2 TEM micrographs of the LDH synthesized via conventional hydrothermal treatment with (a) NaOH and (b) urea; (c) trinal phase hydrothermal system with urea; (d) conventional urea releasing method.

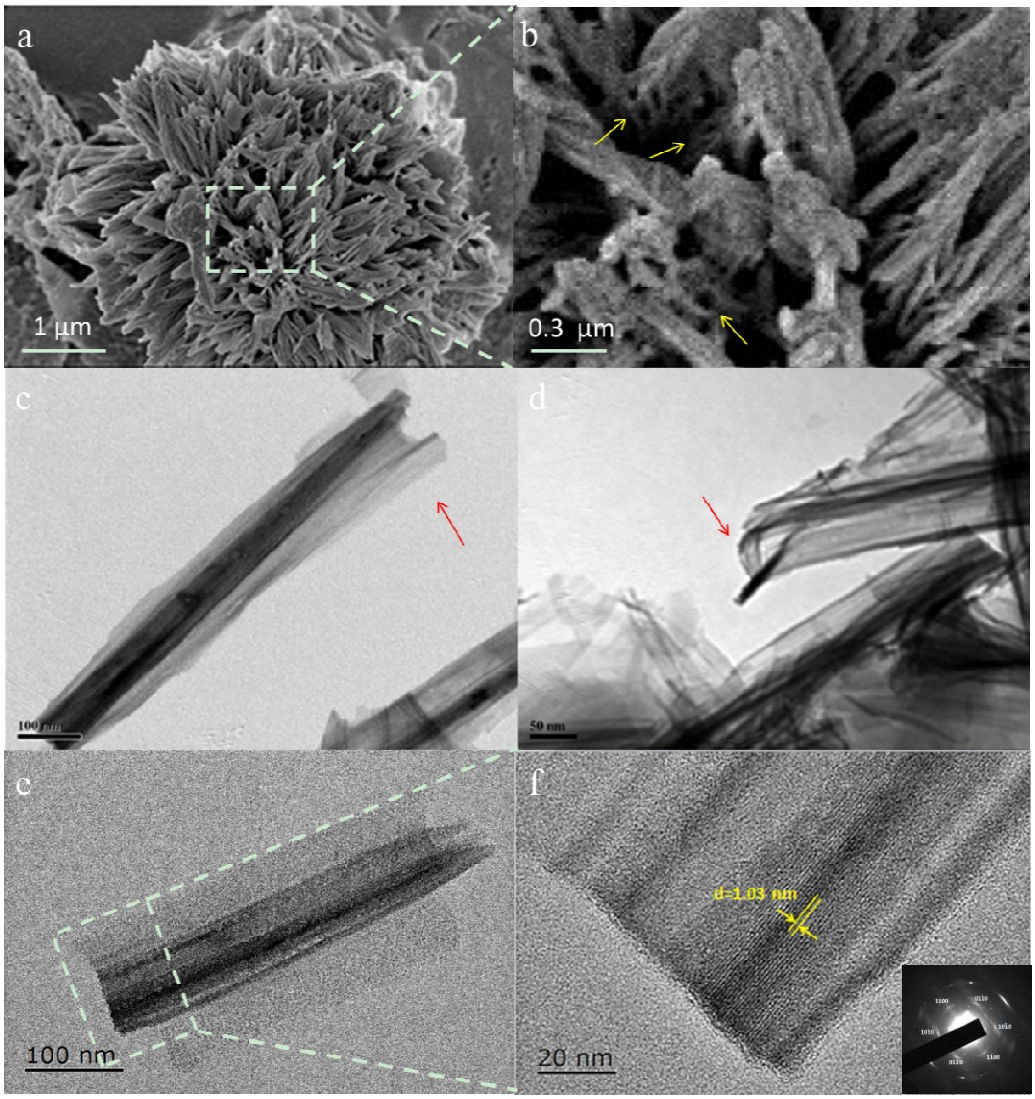

Fig. 3 Different micrographs of the LDH synthesized at 110 °C for 12 h: (a) SEM; (b) magnified SEM image of the dashed-square region in (a); (c,d) TEM; (e) HRTEM; (f) magnified HRTEM image of the dashed-square region in (e). The inset in (f) is an SAED pattern of the LDH nanoscrolls.

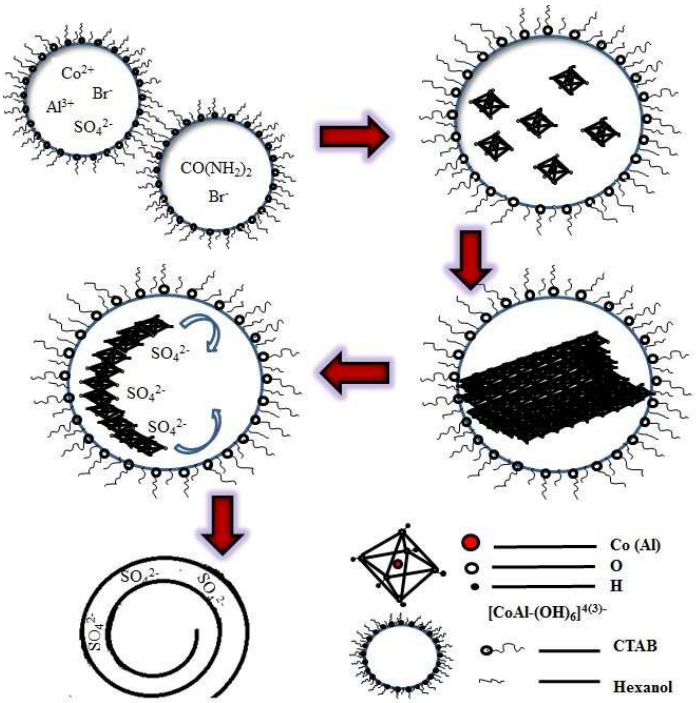

Scheme. 1 Schematic representation of the nucleation and structural evolution process of the LDH nanoscrolls.

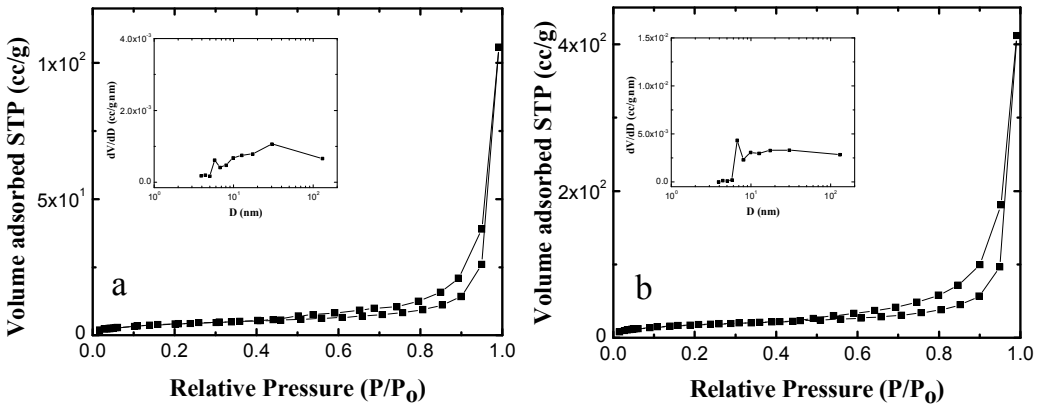

Fig. 4 Nitrogen adsorption-desorption isotherms of the LDH synthesized via (a) conventional urea releasing method and (b) trinal-phase hydrothermal system. The insets in (a) and (b) are the pore size distribution of the two samples respectively.

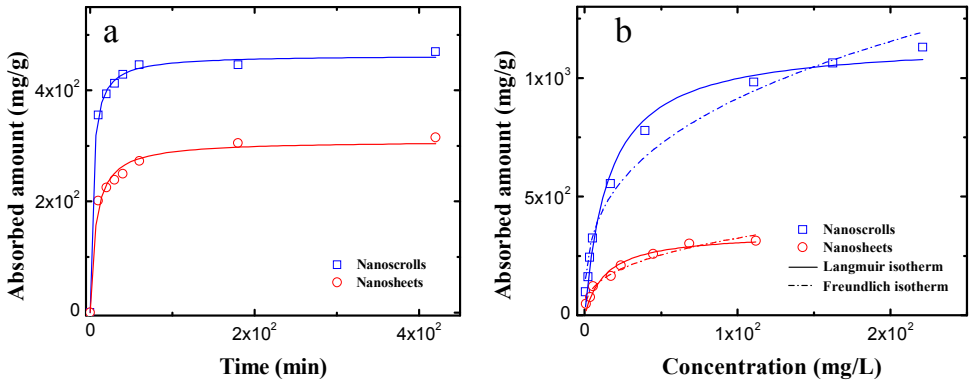

Fig. 5 (a) MO uptake (300 mg/L at time zero) by LDH nanosheets and nanoscrolls as a function of time at 30 °C. The symbols are for the experimental data, and the curves were calculated by fitting the data according to the pseudo-second-order model; (b) adsorption isotherms of MO dye on LDH nanosheets and nanoscrolls at 30 °C.

Table 1 Textural properties of the LDH samples synthesized via two methods.

Samples / Parameters	Nanosheets	Nanoscrolls
Specific surface area (m^2/g)	15.43	63.49
Pore diameter (nm)	42.44	40.11
Pore volume (cm^3/g)	0.1638	0.6367

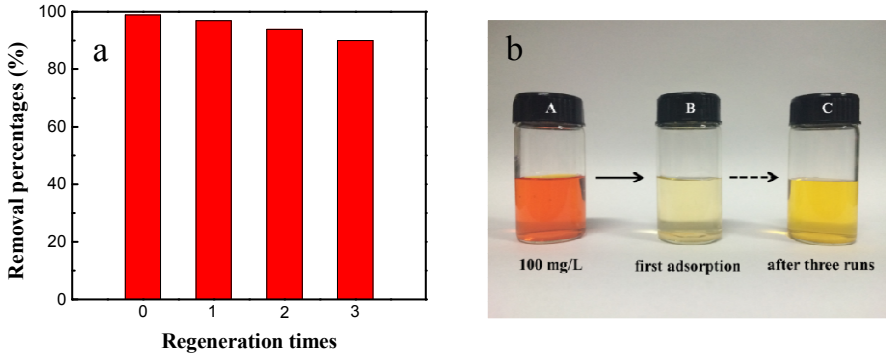

Fig. 6 (a) The removal efficiency of MO by adsorption using the LDH nanoscrolls in different recycle runs; (b) Optical image taken after MO dye adsorption with the different recycle runs.

Formation Mechanism of Layered Double Hydroxide Nanoscrolls by Facile Trinal-Phase Hydrothermal Treatment and Their Adsorption Properties

Weiyang LV, Miao DU*, Weijuan YE, Qiang ZHENG

A facile trinal-phase hydrothermal treatment method is developed for fabricating uniform layered double hydroxide nanoscrolls, which exhibit excellent performance for adsorbing methyl orange in aqueous solution.

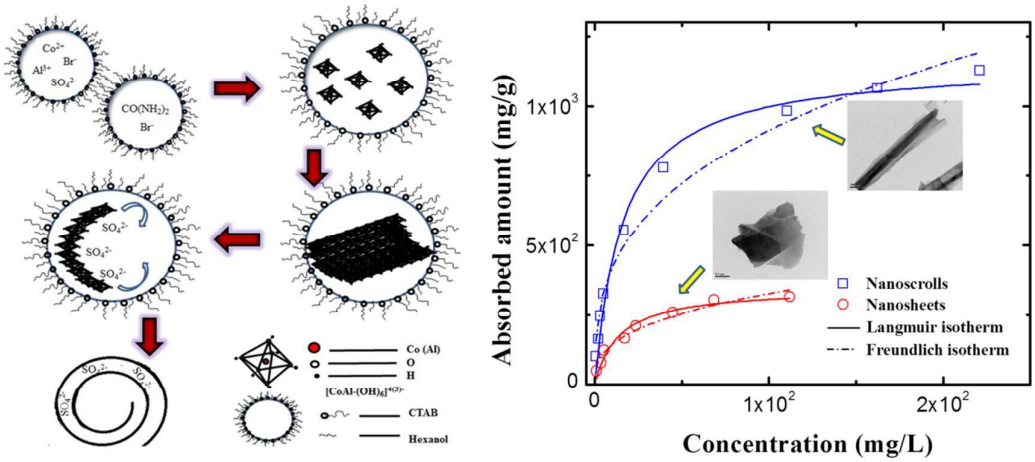

*Corresponding author. E-mail: dumiao@zju.edu.cn, Tel.&Fax: 0086-571-87953075